OXFORD

O R I G I N A L   A R T I C L E

Myelin Pathology Beyond White Matter in Tuberous Sclerosis Complex (TSC) Cortical Tubers

Angelika Mühlebner, MD, PhD, Jackelien van Scheppingen, PhD, Andrew de Neef, MD,
Anika Bongaarts 🆔, MSC, Till S. Zimmer, MSC, James D. Mills, PhD, Floor E. Jansen, MD, PhD,
Wim G.M. Spliet, MD, Pavel Krsek, MD, PhD, Josef Zamecnik, MD, Roland Coras, MD,
Ingmar Blumcke, MD, Martha Feucht, MD, Theresa Scholl, PhD, Victoria-Elisabeth Gruber, MSC,
Johannes A. Hainfellner, MD, Figen Söylemezoğlu, MD, PhD, Katarzyna Kotulska, MD, PhD,
Lieven Lagae, MD, PhD, Anna C. Jansen, MD, PhD, David J. Kwiatkowski, MD, PhD,
Sergiusz Jozwiak, MD, PhD, Paolo Curatolo, MD, PhD, and Eleonora Aronica, MD, PhD

Abstract

Tuberous sclerosis complex (TSC) is a monogenetic disease that arises due to mutations in either the *TSC1* or *TSC2* gene and affects multiple organ systems. One of the hallmark manifestations of TSC are cortical malformations referred to as cortical tubers. These tubers are frequently associated with treatment-resistant epilepsy. Some of these patients are candidates for epilepsy surgery. White matter abnormalities, such as loss of myelin and oligodendroglia, have been described in a small subset of resected tubers but mechanisms underlying this phenomenon are unclear. Herein, we analyzed a variety of neuropathologic and immunohistochemical features in gray and white matter areas of resected cortical tubers from 46 TSC patients using semi-automated quantitative image analysis. We observed divergent amounts of myelin basic protein as well as numbers of oligodendroglia in both gray and white matter when compared with matched controls. Analyses of clinical data indicated that reduced numbers of oligodendroglia were associated with lower numbers on the intelligence quotient scale and that lower amounts of myelin-associated oligodendrocyte basic protein were associated with the presence of autism-spectrum disorder. In conclusion, myelin pathology in cortical tubers extends beyond the white matter and may be linked to cognitive dysfunction in TSC patients.

Key Words: Cognitive dysfunction, Epilepsy, Myelin, Tuberous sclerosis complex, White matter.

INTRODUCTION

According to the World Health Organization (WHO) epilepsy is one of the most common neurologic diseases affecting ∼70 million people worldwide. Although ∼2/3 of all epileptic patients respond well to drug treatment, >30% of cases are drug-resistant [1]. Epilepsy surgery is a highly effective treatment in about one third of these patients [2]. For those who are not surgical candidates, new treatment strategies are urgently needed. Studies that attempt to uncover the molecular basis of epileptic seizures, epileptogenesis and associated neuropsychiatric comorbidities are of utmost importance [3, 4]. Patients with tuberous sclerosis complex (TSC) have been

found to respond even worse to antiepileptic drugs and in these patients presurgical evaluation is increasingly performed (5, 6). TSC is a relatively rare genetic disorder with an estimated prevalence of between 1 in 6800 and 1 in 15 000 newborns (7). Mutations in 2 genes, *TSC1* and *TSC2*, are responsible for the pathological constitutive activation of the highly conserved mechanistic target of rapamycin (mTOR) pathway. Mutations in these genes lead to the development of benign tumors in almost all organ systems, including the subependymal giant cell astrocytoma, cortical tubers, and neuronal migration lines in the brain (8).

Furthermore, cortical tubers are thought to be the pathological substrate of the treatment resistant epilepsy occurring in ∼90% of TSC patients (9, 10). By magnetic resonance imaging (MRI), the classical features of a thickened cortex and fuzzy border between gray white matter including the lack of white matter in the affected area can be seen. These radiological features correlate highly with the epileptogenic tubers removed in surgical candidates (6, 11–13).

Cortical tubers associated with intractable seizures are dynamic and heterogenous lesions and 3 different tuber patterns were recently described (14). Type A cortical tubers are defined by the presence of low-density giant cells and dysmorphic neurons, whereas type B shows a markedly higher density of abnormal cells. In type C, additional calcifications are present. In 2 out of 3 subgroups (tuber type B and C) the white matter is affected. However, the mechanism behind the evident lack of myelin and its clinical implication is poorly understood (14).

Impairment of the fragile myelination process can have a major impact on brain function, in the worst case leading to distorted or interrupted neurotransmissions. It is still unclear whether the observed myelin pathology in epilepsy surgical specimens is primarily related to the underlying malformation process or is a secondary phenomenon of recurrent epileptic seizures (15–17). Interestingly, mTORC1 has been implicated as key signal for myelination, thus, promoting the maturation of oligodendrocytes, the myelin producing cells (18). Recent studies in a limited number of TSC samples have identified a link between myelin reduction and a lower number of oligodendrocytes and its precursors, supporting the hypothesis that myelin reduction is an intrinsic component of the pathological processes (19). These results, however, remain controversial. Shepherd et al indicated an association between white matter reduction and duration of epilepsy and studies in patients with temporal lobe epilepsy and mild malformations of cortical development showed an increased number of oligodendroglia compared with controls (16, 20). Hypomyelination and alteration of oligodendroglia in the prefrontal cortex have been reported as neuropathological hallmarks of autism spectrum disorder (ASD) (21).

In this study, we aim to characterize myelin pathology in relation to clinical manifestations utilizing a battery of semi-automated quantification strategies to investigate whether there is a correlation between affected gray and white matter areas and neuropsychiatric comorbidities.

MATERIALS AND METHODS

Subjects

We evaluated 46 anatomically well preserved tubers from resected neocortical tissue (Department of Pediatric Neurology, Brain Center, University Medical Center Utrecht; Department of Pediatric Neurology, Charles University, Second Faculty of Medicine, Charles University, Motol University Hospital, Prague, Czech Republic and Department of Pediatrics, Medical University Vienna; Department of Neuropathology, University Hospital Erlangen; Department of Pathology, Hacettepe University Ankara; median age at resection = 6.00 years; range = 0.1–47 years; localization: 20 frontal, 13 temporal, 7 parietal, 5 occipital, and 1 hemispheric; gender: 27 males, 19 females). Extensive presurgical evaluation including 24 hours to 5 days video-EEG monitoring, high-resolution MRI and neuropsychological testing was performed in each patient in order to localize the epileptogenic zone, and to identify the target area or lesion for tailored surgical resection. Only if all gathered data were congruent with one epileptogenic tuber was this tuber resected. We also included 9 perituberal samples that were defined by absence of dysmorphic neurons and giant cells on histology (whole tissue blocs were used to ensure equality in available gray and white matter).The age- and localization-matched control group consisted of 34 autopsy cases and 5 surgical samples (median age = 12.00 years; range = 0.1–21 years; localization: 12 frontal, 10 temporal, 9 occipital; gender: 19 males, 20 females). The surgical cases consisted of neocortex exhibiting no signs of tumor infiltration resected in patients with brain tumors and no history of seizures. All postmortem samples were collected within 24 hours of death. None of these patients had a history of seizures or other neurological diseases. All control samples were collected from the Amsterdam University Medical Centers, The Netherlands and the Medical University of Vienna, Austria.

Tissue was obtained and used in accordance with the Declaration of Helsinki and the AMC Research Code provided by the Medical Ethics Committee and approved by the science committee of the UMC Utrecht Biobank. This study was also approved by the Ethical Committee of the Medical University of Vienna and the Ethical Committee of the Motol University Hospital in Prague. Written informed consent was obtained from all patients included in our study.

Tissue Preparation and Immunohistochemistry Protocols

The tissue was carefully oriented, cut perpendicular to the pial surface, fixed overnight in 4% formaldehyde and routinely processed into liquid paraffin. Sections were cut at 4–6-μm with a microtome (Microm, Heidelberg, Germany), and mounted on positively charged slides (Superfrost + Menzel, Germany). Each specimen was histopathologically examined using hematoxylin and eosin (H&E). An immunohistochemical examination of all surgical specimens was performed using

the following panel of antibodies: Oligodendrocyte lineage transcription factor 2 ([olig2], 1:100 dilution, IBL, Minneapolis, MN), neuronal nuclei [NeuN], 1:100, clone A60, Chemicon, Billerica, MA), phosphorylated neurofilament H ([SMI31], 1:1000, clone SMI31, Sternberger, Lutherville, MD), glial fibrillary acidic protein ([GFAP], 1:4000, Dako, Glostrup, Denmark), cluster of differentiation 3 ([CD3], 1:200, clone F7.2.38, DAKO), human leukocyte antigen class II ([HLA-DP, DR, DQ], 1:100, clone Cr3/43, DAKO), phosphorylated S6-ribosomal protein ([pS6], 1:1200, Ser235/236, Cell Signaling Technology, Danvers, MA), myelin basic protein ([MBP], 1:400, DAKO), vimentin (1:500, clone V9, Dako), myelin-associated oligodendrocyte basic protein ([MOBP], 1:50; polyclonal rabbit; HPA035152, Sigma, St. Louis, MO), and programmed cell death 1 ([PD-1], 1:400, Abcam, Cambridge, UK). Autopsy cases were pretreated with 1% Triton X-100 for 1 hour prior to incubation with anti-olig2 antibody. The slides were air-dried overnight at 37°C. All immunohistochemical stainings were performed with a Ventana semiautomated staining machine (Benchmark ULTRA; Ventana, Illkirch, France) and the Ventana DAB staining system according to the manufacturer's protocol.

For double labeling for the detection of regulatory T-cells 3 TSC cases were selected. Sections were deparaffinized in xylene, and ethanol (100%, 95%, 70%) and incubated for 20 minutes in 0.3% H_2O_2 in methanol to block residual tissue peroxidase activity. Antigen retrieval was performed in 0.01 M sodium citrate buffer (pH 6.0) at 121°C for 10 minutes in a pressure cooker. Slides were washed with phosphate-buffered saline ([PBS]; 0.1 M, pH 7.4) and incubated overnight at 4°C with primary antibody in antibody diluent (VWR International, Radnor, PA) against CD25 (ready-to-use, mouse monoclonal, clone 4C9, Leica Biosystems, Buffalo Grove, IL). The following day tissue was washed with PBS and treated with postantibody blocking BrightVision⁺ system (containing rabbit antimouse IgG; Immunologic, Duiven, the Netherlands). Sections were washed with PBS and then developed using 3'-amino 9'-ethylcarbazole ([AEC], Sigma-Aldrich). Color development was stopped by washing slides in deionized water. Incubation with the second primary antibody against forkhead box P3 ([FOXP3], 1:200, monoclonal mouse, clone 236A/E7, Abcam) at 4°C overnight and the next day incubated with BrightVision poly-alkaline phosphatase (AP) antimouse (Immunologic) for 30 minutes at room temperature. AP activity was visualized with the AP substrate kit III Vector Blue (SK-5300, Vector Laboratories Inc., Burlingame, CA). Slides were washed in deionized water and mounted.

Immunofluorescence

Sections were deparaffinated in xylene, rinsed in ethanol (100%, 95%, 70%) and antigen retrieval was performed using a pressure cooker in 0.01 M sodium citrate buffer (pH 6.0) at 120°C for 10 minutes. Slides were then washed with PBS, pH 7.4 and incubated with 10% normal goat serum for 30 minutes at room temperature. Primary antibody for contactin-associated protein ([CASPR], 1:2500, ab34151, Abcam) in Normal Antibody Diluent (Immunological) was incubated overnight at 4°C. Sections were washed in PBS (3× 10 minutes) and incubated for 2 hours at room temperature in goat anti-rabbit IgG-Alexa Fluor 488 (1:200, Invitrogen, Breda, The Netherlands) Coverslips were mounted with Vectashield with DAPI (H-1200, Vector Laboratories, Burlingame, CA). Fluorescent microscopy was performed using Leica Confocal Microscope TSC SP-8X (Leica, Son, The Netherlands).

Semiquantitative Measurements

Slides were scanned at 400× magnification with an Olympus dotSlide system (vs 2.5, Olympus, Tokyo, Japan) in Amsterdam and with the NDPview software (Hamamatsu, NanoZoomer) in Vienna. Scans were exported as a homogeneous set of pyramidal .BIGTIFF files to ensure equality of resolution between the 2 scanners. Stacked images were converted using the bioformat tool of ImageJ2 into single 8-bit RGB files. The DAB-positive area was separated from background using an adjusted protocol for segmentation. Regions of interest (ROI) were selected in order to separate gray from white matter. White matter was considered minimum 500 μm away from the gray-white matter border ([15]). In tuber specimens only affected white matter (based on visual inspection) was selected. All stacks of images were submitted to a batch processing algorithm that was kept consistent throughout the whole analysis.

Cellular Densities

For the calculation of cellular densities, the available images were split into RGB channels. To establish the positive count, a brightness threshold in the blue channel was determined for each staining and size ranges were defined to allow more accurate counts. These parameters were kept the same throughout the analysis and were also implemented in the batch processing algorithm. For quantification of GFAP, SMI31, MBP, MOBP, pS6, vimentin, and Cr3/43 values are expressed in percentage (%) positivity in relation to the total ROI area, meaning that 0% equals no traces of DAB positivity within a specific ROI and 100% when all of the ROI stains positive with DAB. All other cellular densities (CD3, olig2, and NeuN) are represented as total number/mm². CASPR immunofluorescence staining was assessed using integrated optical density measurement. FOXP3/CD25 and PD-1 were inspected visually since presence of positivity was below detection rate.

Clinical Data

The following clinical data were obtained from each participating center: *TSC1/TSC2* mutation status, gender, localization of the resected area, age at epilepsy onset, mean seizure frequency (daily-weekly-monthly), antiepileptic drug management at surgery, type of epilepsy surgery (extent and localization), duration of active epilepsy, and last available postsurgical seizure outcome according to Engel's score. All patients were assessed according to local epilepsy surgery programs including the local battery of age-specific neuropsychological tests. The data were therefore analyzed retrospectively

and as consensus agreed to use average intelligence quotient ([IQ], Wechsler Intelligence Scale for adults and children [WAIS-IV and WISC-V], assessed in values and categories) and presence/absence of ASD as part of the umbrella term TSC-associated neuropsychiatric disorder (TAND) (22–25).

Statistical Analysis

Statistical analysis was performed on SPSS 21 (IBM, PASW Statistics). Due to the lack of normality and nonequality of variances, nonparametric testing (independent-sample Kruskal-Wallis test, Mann-Whitney-*U* test) as well as Kendall-tau correlation were used to analyze the data. Partial correlation was applied if data needed to be corrected for another variable. The Chi-squared test was used for analyzing categorical data. In order to correlate categorial with continuous data the continuous data (MOBP) were divided into 4 subclasses based on quartiles. Bootstrapping was conducted on 1000 samples with bias-corrected and accelerated confidence intervals. p values were considered significant if <0.05.

RESULTS

Overall Neuropathologic Characteristics of Gray and White Matter in TSC Cortical Tuber

Previous studies have focused on the assessment of neuropathological hallmarks within the whole abnormal tissue (for details see [14]). Therefore, as a first step we were interested in the commonalities and differences of standard neuropathology markers between gray and white matter of TSC cortical tubers compared with non-neurologic controls and perilesional tissue. As previously described, there was overall loss of neurons throughout the affected gray matter (NeuN, $p = 0.001$). A subsequent pairwise comparison of type B and type C cortical tubers to controls showed a significant loss of neurons (NeuN, type B: $p = 0.001$; $H = 29.773$; type C: $p = 0.004$; $H = 27.314$). Additionally, we observed an increase in neurons in the white matter in all tuber types and the perituberal samples (NeuN, $p = 0.001$). Furthermore, we observed an increase in number of T-cells present in the gray and white matter (CD3, $p = 0.011$ and $p = 0.009$). The pairwise comparisons showed that the gray matter area of type B tubers was most affected (CD3, type B: $p = 0.045$, $H = -20.982$) with the type C just revealing a tendency when compared with controls (CD3, $p = 0.057$, $H = -20.657$) whereas the white matter areas were significantly different in both types (CD3, type B: $p = 0.028$, $H = -22.107$; type C: $p = 0.009$, $H = -24.857$). However, microglial activation did not reach significance (Cr3/43, gray matter: $p = 0.144$; white matter: 0.548). There was significantly more astrogliosis in the gray matter of all tuber types when compared with the white matter of perituberal samples (GFAP, gray matter: $p = 0.006$; white matter: 0.255). Interestingly, the number of oligodendroglia (olig2-positive cells) and the overall myelin content (MBP positivity) was divergent in both compartments as described below. All findings are summarized in Table.

The Amount of MBP and Numbers of Olig2-Positive Cells Are Altered in Gray and White Matter

Based on our results there was a significant reduction of olig2-positive cells in gray and in white matter (olig2; gray matter: $p = 0.002$; white matter: $p = 0.001$; Fig. 1). After pairwise comparison the perituberal cortex, type A tubers and type B tubers remain significant compared with controls (olig2, perituberal: $p = 0.008$, $H = 30.000$; type A tubers: $p = 0.033$, $H = 21.900$; type B tubers: $p = 0.030$, $H = 19.312$; Fig. 1). This is in contrast to the white matter where mostly type B and C tubers were affected (olig2, type B tubers: $p = 0.007$, $H = 23.972$; type C tubers: $p = 0.043$, $H = 20.630$). Interestingly, the number of olig2-positive cells in the white matter was negatively associated with the presence of calcification (Chi-square; $p = 0.027$; data not shown). Furthermore (as described previously), the amount of myelin within the white matter was reduced (MBP; $p < 0.001$). Pairwise comparison of the tuber types showed a significant myelin reduction in all 3 tuber types compared with controls and perituberal samples (MBP; type A tubers: $p = 0.005$, $H = 27.793$; type B tubers: $p = 0.026$, $H = -29.741$; type C tubers: $p < 0.001$, $H = 40.893$; Fig. 1). Next, the amount of MBP immunopositivity was significantly associated with the presence of calcification (Chi-square; $p = 0.002$, data not shown). These findings were also reflected in the amount of MOBP immunopositivity, which was also significantly reduced in white matter of all tuber types (MOBP, $p = 0.002$, data not shown).

Reductions of Oligodendrocytes and MBP Are Associated with the Presence of Markers of Neuroinflammation

Subsequently, we wanted to explore if there is a connection between our histological parameters and the aberrant number of components of white matter. Therefore, we performed correlation analysis corrected for age at surgery since the age of the patients was in itself significantly correlated with the numbers of olig2-positive cells and MBP positivity (Kendall tau-b). A significant association was found between the reduction of MBP in the white matter and the presence of CD3-positive T-cells in the white matter and the gray matter (partial correlation; white matter: $p < 0.001$; gray matter: $p < 0.001$). Furthermore, the same association was found between CD3-positive T-cells in the gray matter and numbers of oligodendroglia in gray and white matter (olig2; partial correlation; gray matter: $p = 0.027$; white matter: $p = 0.010$). In accordance, the numbers of white matter T-cells negatively correlated with the numbers of olig2-positive cells (partial correlation; gray matter: $p = 0.012$; white matter: $p = 0.001$; Fig. 2). Interestingly, also the presence of activated microglia correlated with a reduced number of oligodendroglia in the gray matter (partial correlation; $p = 0.008$). All other parameters did not reach significance when corrected for age.

Based on recent results we explored the possible involvement of regulatory T-cells in the pathogenesis of hypomyelination. We were only able to detect single PD-1-positive cells scattered throughout the gray and white matter. A few more

TABLE. Overview of the Quantitative Analysis

		Control					Type A Cortical Tuber					Type B Cortical Tuber					Type C Cortical Tuber					Perituberal Cortex					Statistical Significance
Measurement	Region	Total Available n	n	Median	Min	Max	Total Available n	n	Median	Min	Max	Total Available n	n	Median	Min	Max	Total Available n	n	Median	Min	Max	Total Available n	n	Median	Min	Max	p Value
T-cells/mm² [CD3]	Gray matter	39	7	2.78	0.45	3.54	11	11	4.12	1.00	22.07	20	16	11.26	0.64	43.69	15	15	11.34	0.26	76.52	9	7	2.77	0.98	6.84	**0.011**
T-cells/mm² [CD3]	White matter	39	7	4.22	0.80	9.70	11	11	13.76	0.33	31.66	20	16	20.47	3.59	80.94	15	15	17.77	1.96	128.96	9	7	12.71	1.46	32.04	**0.011**
Neurons/mm² [NeuN]	Gray matter	39	7	1499.90	1059.00	1842.73	11	11	909.64	227.98	1491.58	20	17	548.63	125.10	1404.76	15	15	550.64	224.04	1805.36	9	8	942.93	406.39	1521.70	**0.001**
Neurons/mm² [NeuN]	White matter	39	7	1.60	0.20	10.40	11	11	38.44	9.65	123.71	20	17	51.78	5.63	864.08	15	15	35.94	10.80	147.40	9	8	46.15	10.52	123.40	**0.001**
Microglial activation % [Cr3/43]	Gray matter	39	7	0.88	0.17	2.12	11	11	0.61	0.09	30.37	20	16	2.33	0.39	26.66	15	15	2.23	0.04	18.91	9	9	0.71	0.01	9.05	0.144
Microglial activation % [Cr3/43]	White matter	39	7	0.92	0.52	3.91	11	11	1.49	0.44	7.68	20	16	2.84	0.50	12.04	15	15	2.33	0.10	14.02	9	9	1.35	0.76	5.45	0.548
Gliosis % [GFAP]	Gray matter						11	9	2.40	0.09	44.21	20	17	19.87	0.27	56.04	15	15	12.52	1.43	73.13	9	8	1.42	0.10	12.08	**0.006**
Gliosis % [GFAP]	White matter						11	9	27.97	4.11	88.15	20	17	18.41	4.71	64.93	15	15	11.59	1.34	62.49	9	8	13.31	5.93	56.73	0.255
Oligodendroglia/mm² [olig2]	Gray matter	39	18	243.50	158.88	394.88	11	10	80.42	29.68	477.66	20	16	85.06	32.54	449.56	15	15	122.47	56.03	520.68	9	6	83.23	23.13	120.35	**0.002**
Oligodendroglia/mm² [olig2]	White matter	39	31	517.00	249.66	681.50	11	10	412.36	145.02	624.94	20	16	234.40	89.92	818.71	15	15	237.28	95.03	895.57	9	7	590.11	176.37	907.39	**0.001**
Myelin % [MBP]	Gray matter	39	14	0.11	0.00	10.37	11	9	0.51	0.07	1.73	20	15	1.79	0.02	9.01	15	14	0.81	0.08	9.35	9	7	1.06	0.43	6.45	0.106
Myelin % [MBP]	White matter	39	28	93.36	56.98	99.00	11	10	44.62	0.80	84.76	20	16	11.24	0.03	79.77	15	14	7.76	0.13	61.64	9	7	73.02	65.34	90.01	**<0.001**
Myelin 2% [MOBP]	Gray matter	39	4	4.96	3.05	5.73	11	2	1.31	1.01	1.60	20	6	10.55	0.05	25.49	15	4	12.32	6.88	18.70	9	2	3.43	3.20	3.66	0.086
Myelin 2% [MOBP]	White matter	39	15	68.00	7.00	100.00	11	2	27.03	16.93	37.13	20	6	4.01	0.05	17.12	15	4	2.28	0.81	18.26	9	2	15.05	0.44	29.66	**0.002**
axons % [SMI31]	White matter	39	7	67.30	24.10	77.70	11	4	53.91	29.91	58.60	20	2	30.04	24.97	35.10	15	2	47.73	41.80	53.66	9	3	34.65	23.41	83.43	0.126
Nodes of Ranvier IOD [CASPR]	White matter	39	5	5648.66	1831.33	9305.75	11					20	2	1483.77	956.88	2010.66	15	3	1368.21	1129.60	1563.58	9					**0.016**

All values are represented in median, minimum, and maximum. The total number of cases within the subgroup is shown as well as the number of cases available for the specific analysis. Significance level shown based on Kruskal-Wallis test except for [SMI31] and [CASPR], these are based on Mann-Whitney-*U* testing. Values considered significant < 0.05. GM, gray matter; WM, white matter; olig2, oligodendroglia; MOBP, myelin associated oligodendrocyte basic protein; MBP, myelin basic protein; GFAP, glial fibrillary acidic protein; n, number; min, minimum; max, maximum.
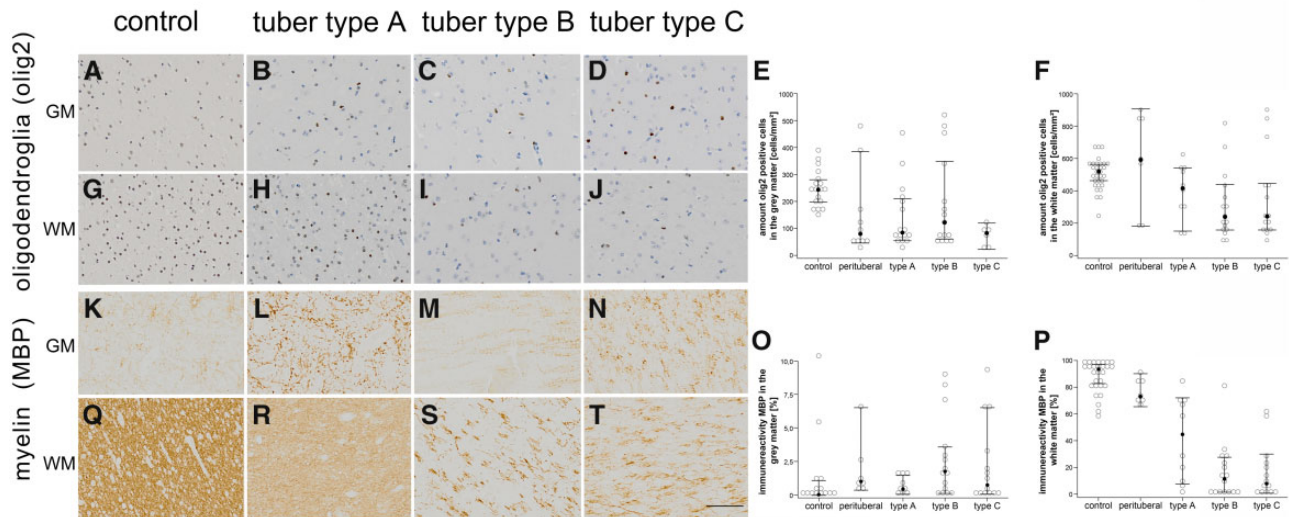
FIGURE 1. Oligodendroglia and myelin are affected in TSC cortical tubers. **(A–D)** Representative histological slides of gray matter in control **(A)**, type A cortical tuber **(B)**, type B tuber **(C)** and type C tuber **(D)**. **(E, F)** Oligodendroglia are reduced in all tubers compared with control and perilesional samples (olig2; gray matter: p = 0.002; white matter: p = 0.001; Kruskal-Wallis test). The reduction of oligodendroglia in the gray matter was evident among all 3 tuber types after pairwise comparison. However, a reduced number of oligodendroglia in white matter was visible only in the type B and C subtypes (olig2, type B tubers: p = 0.007, H = 23.972; type C tubers: p = 0.043, H = 20.630). In accordance with previous publications 3 main subgroups of oligodendroglial proliferation (high medium and low) were present [19]. **(G–J)** Distribution and numbers of olig2-positive cells within the white matter of controls **(G)**, type A tubers **(H)**, type B tubers **(I)** and type C tubers **(J)**. **(K–N)** Distribution of MBP among gray matter in controls **(K)**, type A tubers **(I)**, type B tubers **(M),** and type C tubers **(N)**. **(O, P)** The amount of myelin within the white matter was reduced (MBP; p < 0.001). Pairwise comparison of the tuber types showed a significant myelin reduction in all tuber types (MBP; type A tubers: p = 0.005, H = 27.793; type B tubers: p = 0.026, H = − 29.741; type C tubers: p < 0.001, H = 40.893; Kruskal-Wallis test). **(Q–T)** Expression pattern of MBP in white matter among controls **(Q)**, type A tubers **(R)**, type B tubers **(S)**, and type C tubers **(T)**. Scale bar in r equals 200 μm and applies also to **A–D, F–I, J–M,** and **O–Q**. Filled dots in **E, F, O,** and P equals median, the whiskers show 95% confidence intervals. MBP, myelin basic protein; WM, white matter; GM, gray matter; olig2, oligodendroglia.

were present inside the blood vessels. Even fewer cells were visible with CD25/FOXP3 double staining (Fig. 2 insert).

Loss of Nodes of Ranvier at the Gray-White Matter Border While the Number of Axons Is Intact

In line with previous studies, our findings support the hypothesis of the use of the term "dysmyelination" in epilepsy cases. Our next step was to determine whether the myelin abnormalities were due to the absence of axons. However, this was not the case. There was no difference in the amount of phosphorylated neurofilament (SMI31) among the stained subgroups (Mann-Whitney-*U*; white matter: p = 0.126). Subsequently, we performed immunofluorescence staining of CASPR as a subunit of the nodes of Ranvier in a subset of cases (n = 5) to assess the presence of properly myelinated axons. Here, we saw a reduction of CASPR positivity at the gray-white matter border of type B and type C cortical tubers (Mann-Whitney-*U*; p = 0.016; Fig. 3).

Parameters of Cognitive Functioning Correlate With Numbers of Oligodendroglia and Specific Myelin Components

We tested a range of acquired clinical variables typically assessed during presurgical evaluation and tested them against

our neuropathological parameters. We received 28 complete clinical data sets and only information on ASD/TAND status of another 4 patients. The numbers of oligodendroglia in the white matter were significantly associated with the level of IQ at surgery whereas the same trend was seen regarding oligodendroglia in the gray matter (Kendall-tau *b*; gray matter: p = 0.071; white matter: p = 0.023; Fig. 4A). Twenty-two patients were seizure-free one year after surgery (Engel score 1). Furthermore, the presence of ASD/TAND was associated with the amount of immunopositive MOBP in the gray matter (Chi square; p = 0.007; Fig. 4B). White matter MOBP content failed to reach significance level (Chi square; p = 0.057). There was no association with any other of the patients' clinical characteristics including antiepileptic drug therapy (Supplementary Data Table S1).

DISCUSSION

The present study investigated whether myelin pathology extends from white matter to gray matter in cortical tubers of TSC. The following observations were made: (1) the numbers of olig2-positive cells was altered in gray and white matter; (2) myelin loss was evident only in white matter; (3) myelin pathology was associated with the presence of T-cells suggesting an involvement of inflammatory cells in myelin
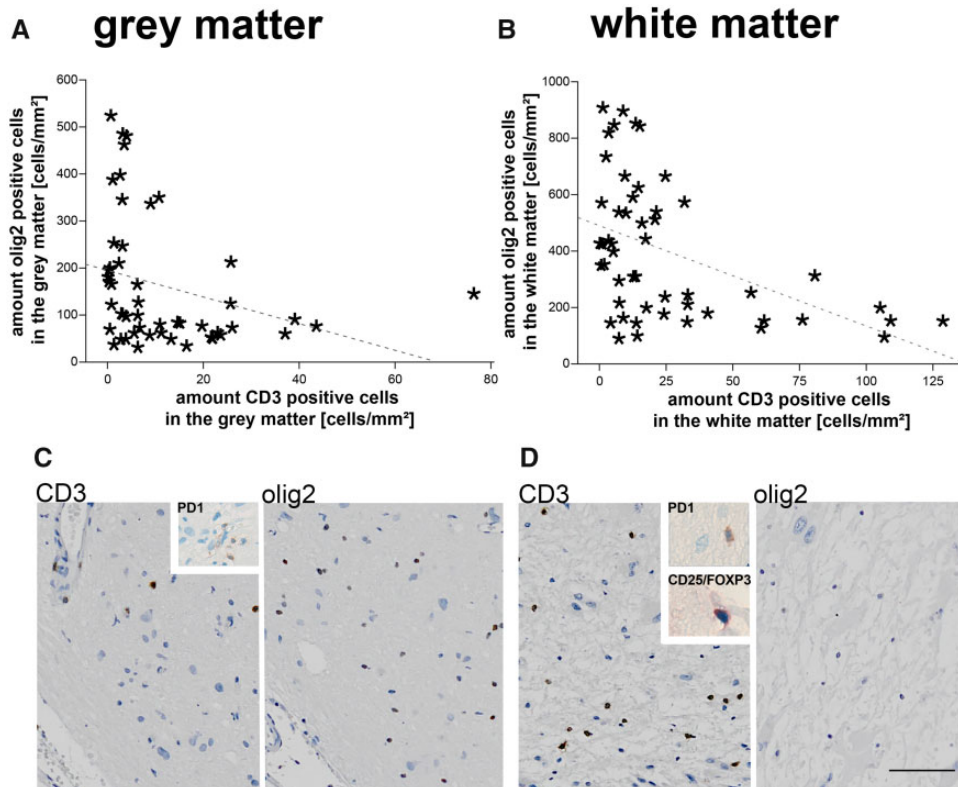
FIGURE 2. The low number of olig2-positive cells correlates with the presence of T-cells. **(A, B)** In the presence of CD3-positive T-cells the numbers of olig2-positive oligodendroglial cells are reduced in gray **(A)** and white matter **(B)** (partial correlation corrected for age; white matter: p = 0.003; gray matter: p < 0.001). The dashed line equals linear relationship with $R^2 = 0.089$ in **A** and $R^2 = 0.216$ in **B**. **(C, D)** Type C cortical tuber showing an increase of CD3-positive T-cells in the gray **(C)** and white matter **(D)** with a corresponding low number of oligodendroglia. Inserts represent scarce single CD25/FOXP3 and PD-1-positive T-cells. Scale bar in d equals 200 μm and applies also to c. WM, white matter; GM, gray matter; olig2, oligodendroglia.

pathology; (4) we identified a loss of nodes of Ranvier at the gray-white matter border without a reduction in the number of axons to reflect deficiency in proper myelin formation, and (5) altered myelin properties were associated with lower levels of cognitive functioning in our cohort of TSC patients with resected cortical tubers. The significance of these findings in TSC in relation to the current understanding of the pathophysiology of myelin biology is discussed below.

mTOR and Oligodendrocyte Maturation

Brain development during prenatal human life is a complicated process involving a number of important cellular regulatory processes that are paramount to gaining the shape and functionality required for the formation of the adult brain (26). White matter expansion and myelination starts at a later stage and continues until the first years after birth. Its regulation is mainly mediated by the number of available axons (27). A density-dependent feedback inhibition of proliferation reduces the responsiveness of the cells to their growth factors and the final matching of oligodendrocyte and axon number is accomplished through the local regulation of cell death (28). Not at all surprising, the mTOR pathway plays a crucial role in central nervous system development and myelination based on its

regulatory functions in metabolism and protein synthesis. After all, myelination is an energy consuming process (18). Nevertheless, mTOR plays a pivotal role in oligodendroglial differentiation as well. Recent data suggest that synergistic contributions of mTORC1 and mTORC2 are essential to drive oligodendroglial differentiation (29). If it fails, apoptosis of oligodendrocytes is a possible consequence (30). In our cohort we observed a reduction of oligodendroglial cells within gray and white matter probably reflecting the ultimate consequence of aberrant mTOR activation including impaired oligodendroglial differentiation as well as a reduced number of neurons—many of which displayed dysmorphic morphology (14, 31). However, an effect of recurrent seizures cannot fully be excluded. Nevertheless, in our cohort there was no association with epilepsy duration or any specific type of seizures.

Neuroinflammation and Oligodendrocyte Maturation

In the present study, we found a negative correlation of inflammatory markers with abnormal myelin suggesting an involvement of the adaptive immune response. However, to date, no signs of classic inflammation-mediated demyelination, as seen in multiple sclerosis, has been found (17, 19).
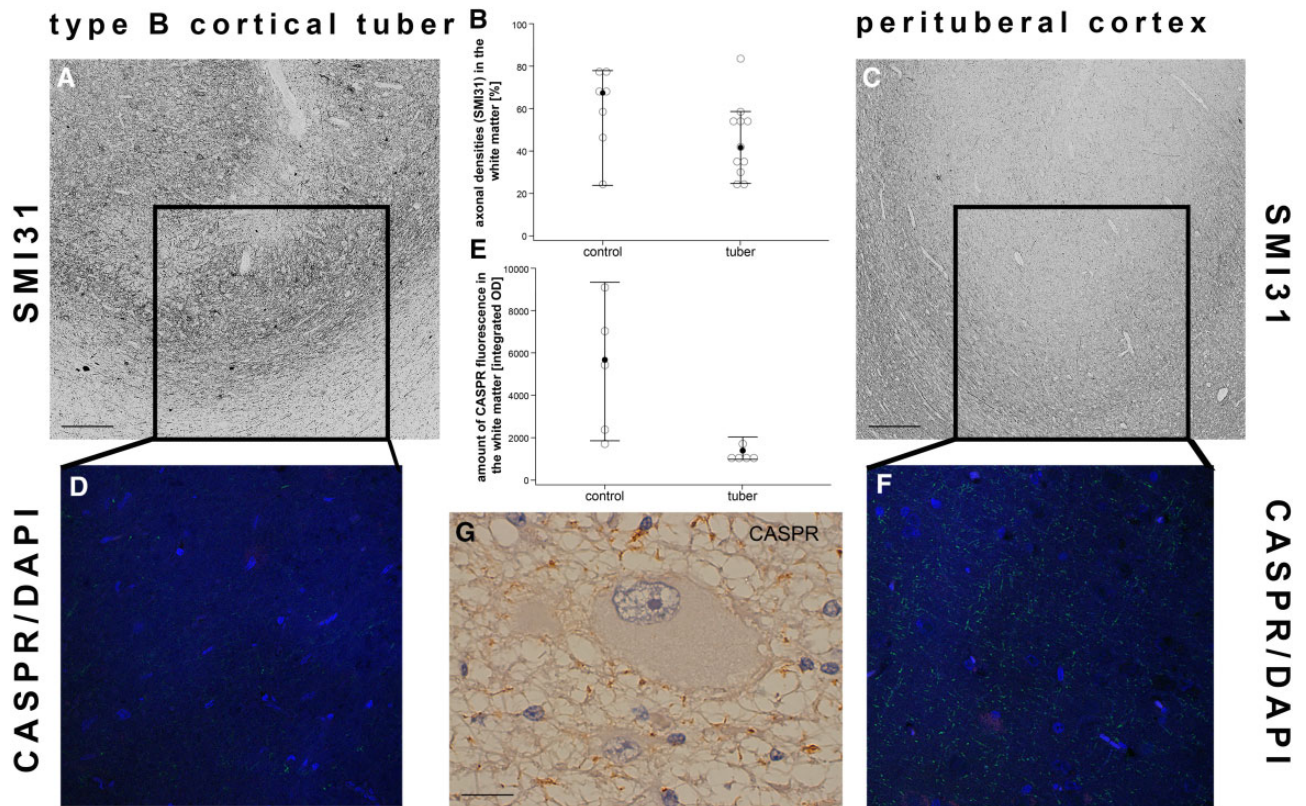
FIGURE 3. Loss of nodes of Ranvier while the number of axons stay intact. **(A)** Cortex of a type B cortical tuber displaying the presence of phosphorylated neurofilament-positive axons (SMI31) at the gray-white matter border with the corresponding loss of CASPR-positive nodes of Ranvier **(D**; CASPR/DAPI**)**. **(B)** No differences in SMI31-positive axons could be detected between the subgroups (white matter: p = 0.126; Mann-Whitney-*U* test). **(C)** Perilesional sample of the same patient as in a showing and normal number of axons (SMI31) and nodes of Ranvier (**F**; CASPR/DAPI) at the gray-white matter border. **(E)** Integrated optical density of CASPR fluorescence is reduced in cortical tubers (Mann-Whitney-*U* test, p = 0.016). Filled dots equal median, whiskers show 95% confidence intervals. **(G)** Abnormal arrangement of nodes of Ranvier in the presence of a giant cell. Scale bar in **A** and **C** equals 200 μm. Scale bar in e equals 25 μm. WM, white matter; GM, gray matter; CASPR, contactin-associated protein.

Thus, the role of T-cells in the context of myelin pathology in TSC requires further investigation in experimental models. Nevertheless, we did not observe an increased number of regulatory T-cells, which might suggest their involvement in the pathogenesis of hypomyelination is rather limited (32). Furthermore, oligodendrocytes show a high capacity of migration and remyelination of naked axons (33). We do not see such attempts in epilepsy surgery specimens of patients with malformations of cortical development (17). However, in selected subgroups oligodendroglial hyperplasia has been reported (17, 20, 34). Therefore, a direct attack of immune-competent cells on the myelin sheath seems unlikely, although the precise role of the immune system in gray and white matter pathology has yet to be unraveled. A complex noxious micro-environment consisting of seizure induced toxicity, mTOR related dysmaturation, gliopathy, blood-brain barrier leakage with extracellular matrix dysfunction and loss of overall neurons seems more likely to contribute to the dysmyelination seen in TSC cortical tubers (19, 35–38). This concept is supported by the idea of myelin dynamics/plasticity. Experimental evidence shows that myelination in the cortex responds to neural activity with enhanced oligodendrocyte integration rather than remodeling existing internodes (39, 40). Additionally, the loss of nodes of Ranvier observed at the gray-white matter border in TSC (without a reduced number of axons) may reflect deficiency in proper integration of postnatal-born oligodendrocytes in response to persistent abnormal neural activity (40, 41).

Gray Matter Oligodendrocytes

Strikingly, recent studies indicate that myelin plasticity occurs through different region-specific mechanisms, and human white matter oligodendrocytes have been shown to have limited turnover during life compared with gray matter oligodendrocytes (42). This is congruent with the current understanding of the diversity of oligodendrocytes and their progenitors, which is also supported by recent single-cell RNA-Seq data analyses, showing specific alterations in oligodendroglial heterogeneity in multiple sclerosis (43, 44). Future experiments using single-cell RNA-Seq analyses could be important to identify specific alterations in oligodendroglial heterogeneity in TSC, guiding a better understanding of patient phenotypic heterogeneity. In our study we observed divergent
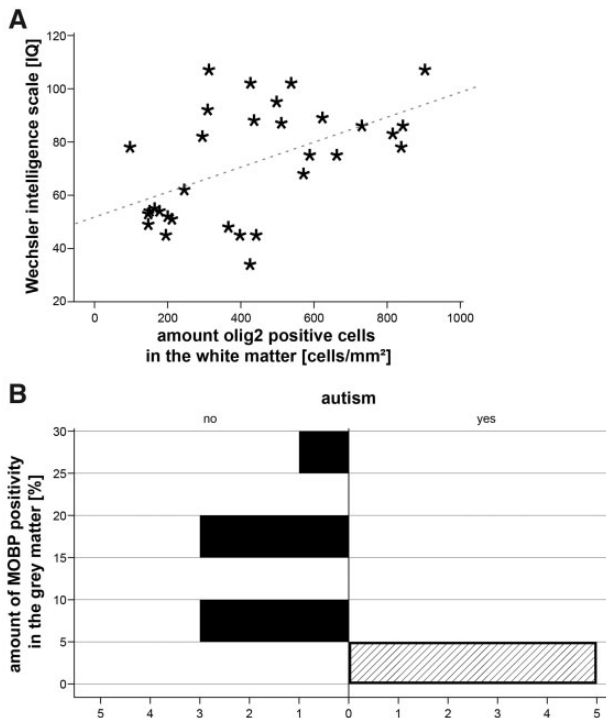
FIGURE 4. The numbers of oligodendroglia and myelin-specific proteins correlate with patient cognitive performance parameters. Population charts. **(A)** Low numbers of oligodendroglia in the white matter correlated with overall cognitive performance of patients at surgery (Kendall-tau b correlation, p = 0.023). Dashed line represents linear relationship with $R^2 = 0.271$. **(B)** The presence of autism spectrum disorder is associated with the amount of MOBP in the gray matter (p = 0.007; Chi square). WM, white matter; GM, gray matter; olig2, oligodendroglia; MOBP, myelin-associated oligodendrocyte basic protein.

amounts of MBP immunoreactivity as well as numbers of oligodendroglia not only in white but also in the gray matter, compared with controls and perilesional cortex. Recently, attention has been focused on gray matter myelination based on the evidence that particularly gray matter oligodendrocytes show a prominent postnatal turnover and continue to be added until the fourth decade (42), contributing to lifelong brain plasticity (45). In focal cortical dysplasia type II, a morphologically similar pathology frequently encountered in epilepsy surgery, myelin sheath formation is compromised in gray matter alongside with reduced numbers of oligodendroglial cells (46). Thus, understanding regulation and function of gray matter myelination in the context of TSC and related mTORopathies deserves further investigation.

Myelin Integrity and Developmental Disorders

Regardless of the underlying pathophysiologic mechanism, alterations of myelin dynamics, depending on their severity, are known to be linked to various kinds of developmental disorders or neuropsychiatric manifestations. Over the past decades, a number of imaging studies

highlighted aberrant white matter tracts to be associated with neuropsychiatric in patients who have long-term epilepsy (47). Especially in TSC, white matter properties on diffusion tensor imaging seem to correlate with neurologic function (48). Furthermore, proper myelin integrity plays a crucial role in human cognitive development (49). Interestingly, in our cohort, IQ was associated strongly with numbers of oligodendrocytes in the white matter and with lower levels in the gray matter. In other words, the lower the numbers of oligodendroglia the worse the global cognitive performance.

One of the neuropsychiatric comorbidities subsumed under TAND, especially if severe epilepsy starts at an early age, is ASD (50). In our cohort of TSC patients who underwent surgery, the amount of immunoreactive MOBP in the gray matter was associated with the presence of autism. The abundance of MOBP resembles that of MBP, a major component of the myelin sheath, in several aspects; it has also been reported to be localized as mRNA and translated in the peripheral myelin compartment (51). MOBP supports oligodendroglial differentiation and the formation of myelin-like membrane sheets (52). A recent study conducting genome-wide transcriptional profiling in a mouse model of neurodevelopmental disorders with induced prenatal immune response revealed that MOBP is among the list of unique and commonly differentially expressed genes in mice offspring affected with cognitive dysfunction similar to schizophrenia or ASD. Moreover, not only MOBP but also other myelin-associated genes were affected, once more stressing the importance of myelin for cognitive function (53). Furthermore, myelin fiber bundles seem to be disconnected on diffusion tensor imaging in early white matter development of TSC patients who develop ASD later in life (54).

We acknowledge that in this study we only focused on TSC. This was done to ensure a common genetic background across all samples and to leverage TSC as model disease for constitutive mTOR pathway activation. No other epilepsy-associated pathologies were included in this study, and it would be interesting to see if the results presented here can be generalized across other epileptic encephalopathies. Furthermore, data retrieval and analysis, especially neuro-psychiatric evaluation, was retrospective across different countries and is therefore far from complete. Additionally, tissue-based analysis only gives insights into this very sensitive equilibrium at a certain moment of brain development and function. Nevertheless, unraveling the mechanism of myelin pathology in conditions of constitutive mTOR activation will help to better understand neuropsychiatric comorbidities in patients with epilepsy.

Rome, Italy: M.M. Antonelli, F. Giangaspero; Institute of Neuropathology, Westfälische Wilhelms—Universität Münster, Münster, Germany: W. Paulus; Department of Neuropathology, Centro Hospitalar Lisboa Norte, EPE, Lisbon, Portugal: J. Pimentel; Department of Human Pathology and Oncology, University of Florence and Division of Neurosurgery, "Anna Meyer" Pediatric Hospital, Florence, Italy: A.M. Buccoliero, F. Giordano.

REFERENCES

1. Kwan P, Schachter SC, Brodie MJ. Drug-resistant epilepsy. N Engl J Med 2011;365:919–26
2. Rosenow F, Luders H. Presurgical evaluation of epilepsy. Brain 2001;124:1683–700
3. Jozwiak S, Becker A, Cepeda C, et al. WONOEP appraisal: Development of epilepsy biomarkers—What we can learn from our patients? Epilepsia 2017;58:951–61
4. Walker LE, Janigro D, Heinemann U, et al. WONOEP appraisal: Molecular and cellular biomarkers for epilepsy. Epilepsia 2016;57:1354–62
5. Liang S, Zhang J, Yang Z, et al. Long-term outcomes of epilepsy surgery in tuberous sclerosis complex. J Neurol 2017;264:1146–54
6. Krsek P, Jahodova A, Kyncl M, et al. Predictors of seizure-free outcome after epilepsy surgery for pediatric tuberous sclerosis complex. Epilepsia 2013;54:1913–21
7. O'Callaghan FJ, Shiell AW, Osborne JP, et al. Prevalence of tuberous sclerosis estimated by capture-recapture analysis. Lancet 1998;351:1490
8. Jones AC, Shyamsundar MM, Thomas MW, et al. Comprehensive mutation analysis of TSC1 and TSC2-and phenotypic correlations in 150 families with tuberous sclerosis. Am J Hum Genet 1999;64:1305–15
9. Chu-Shore CJ, Major P, Camposano S, et al. The natural history of epilepsy in tuberous sclerosis complex. Epilepsia 2009;51:1236–41
10. Curatolo P, Moavero R, de Vries PJ. Neurological and neuropsychiatric aspects of tuberous sclerosis complex. Lancet Neurol 2015;14:733–45
11. Jansen FE, van Huffelen AC, Algra A, et al. Epilepsy surgery in tuberous sclerosis: A systematic review. Epilepsia 2007;48:1477–84
12. Jansen FE, Huiskamp G, Huffelen AC, et al. Identification of the epileptogenic tuber in patients with tuberous sclerosis: A comparison of high-resolution EEG and MEG. Epilepsia 2006;47:108–14
13. Jahodova A, Krsek P, Kyncl M, et al. Distinctive MRI features of the epileptogenic zone in children with tuberous sclerosis. Eur J Radiol 2014;83:703–9
14. Muhlebner A, van Scheppingen J, Hulshof HM, et al. Novel histopathological patterns in cortical tubers of epilepsy surgery patients with tuberous sclerosis complex. PLoS One 2016;11:e0157396
15. Muhlebner A, Coras R, Kobow K, et al. Neuropathologic measurements in focal cortical dysplasias: Validation of the ILAE 2011 classification system and diagnostic implications for MRI. Acta Neuropathol 2012;123:259–72
16. Shepherd C, Liu J, Goc J, et al. A quantitative study of white matter hypomyelination and oligodendroglial maturation in focal cortical dysplasia type II. Epilepsia 2013;54:898–908
17. Zucca I, Milesi G, Medici V, et al. Type II focal cortical dysplasia: Ex vivo 7T magnetic resonance imaging abnormalities and histopathological comparisons. Ann Neurol 2016;79:42–58
18. Figlia G, Gerber D, Suter U. Myelination and mTOR. Glia 2018;66:693–707
19. Scholl T, Muhlebner A, Ricken G, et al. Impaired oligodendroglial turnover is associated with myelin pathology in focal cortical dysplasia and tuberous sclerosis complex. Brain Pathol 2017;27:770–80
20. Schurr J, Coras R, Rossler K, et al. Mild malformation of cortical development with oligodendroglial hyperplasia in frontal lobe epilepsy: A new clinico-pathological entity. Brain Pathol 2017;27:26–35
21. Graciarena M, Seiffe A, Nait-Oumesmar B, et al. Hypomyelination and oligodendroglial alterations in a mouse model of autism spectrum disorder. Front Cell Neurosci 2018;12:517.
22. Engel J Jr. Update on surgical treatment of the epilepsies. Summary of the Second International Palm Desert Conference on the Surgical Treatment of the Epilepsies (1992). Neurology 1993;43:1612–7
23. de Vries PJ, Franz DN, Curatolo P, et al. Measuring health-related quality of life in tuberous sclerosis complex—Psychometric evaluation of three instruments in individuals with refractory epilepsy. Front Pharmacol 2018;9:964.
24. Baxendale S, McGrath K, Thompson PJ. Epilepsy & IQ: The clinical utility of the Wechsler Adult Intelligence Scale-Fourth Edition (WAIS-IV) indices in the neuropsychological assessment of people with epilepsy. J Clin Exp Neuropsychol 2014;36:137–43
25. MacAllister WS, Maiman M, Vasserman M, et al. The WISC-V in children and adolescents with epilepsy. Child Neuropsychol 2019;25:992–1002
26. Jiang X, Nardelli J. Cellular and molecular introduction to brain development. Neurobiol Dis 2016;92:3–17
27. Ffrench-Constant C, Raff MC. The oligodendrocyte-type-2 astrocyte cell lineage is specialized for myelination. Nature 1986;323:335–8
28. Orentas DM, Miller RH. Regulation of oligodendrocyte development. Mol Neurobiol 1998;18:247–59
29. Grier MD, West KL, Kelm ND, et al. Loss of mTORC2 signaling in oligodendrocyte precursor cells delays myelination. PLoS One 2017;12:e0188417
30. Lebrun-Julien F, Bachmann L, Norrmen C, et al. Balanced mTORC1 activity in oligodendrocytes is required for accurate CNS myelination. J Neurosci 2014;34:8432–48
31. Ruppe V, Dilsiz P, Reiss CS, et al. Developmental brain abnormalities in tuberous sclerosis complex: A comparative tissue analysis of cortical tubers and perituberal cortex. Epilepsia 2014;55:539–50
32. Pilipow K, Basso V, Migone N, et al. Monoallelic germline TSC1 mutations are permissive for T lymphocyte development and homeostasis in tuberous sclerosis complex individuals. PLoS One 2014;9:e91952
33. Franklin RJM, Ffrench-Constant C. Regenerating CNS myelin—From mechanisms to experimental medicines. Nat Rev Neurosci 2017;18:753–69
34. Stefanits H, Czech T, Pataraia E, et al. Prominent oligodendroglial response in surgical specimens of patients with temporal lobe epilepsy. Clin Neutopathol 2012;31:409–17
35. Muhlebner A, Bongaarts A, Sarnat HB, et al. New insights into a spectrum of developmental malformations related to mTOR dysregulations: Challenges and perspectives. J Anat 2019;235:521–42
36. Falcao AM, van Bruggen D, Marques S, et al. Disease-specific oligodendrocyte lineage cells arise in multiple sclerosis. Nat Med 2018;24:1837–44
37. Broekaart DWM, Anink JJ, Baayen JC, et al. Activation of the innate immune system is evident throughout epileptogenesis and is associated with blood-brain barrier dysfunction and seizure progression. Epilepsia 2018;59:1931–44
38. Bugiani M, van der Knaap MS. Childhood white matter disorders: Much more than just diseases of myelin. Acta Neuropathol 2017;134:329–30
39. Hughes EG, Orthmann-Murphy JL, Langseth AJ, et al. Myelin remodeling through experience-dependent oligodendrogenesis in the adult somatosensory cortex. Nat Neurosci 2018;21:696–706
40. Swire M, Ffrench-Constant C. Seeing is believing: Myelin dynamics in the adult CNS. Neuron 2018;98:684–6
41. Bechler ME, Swire M, Ffrench-Constant C. Intrinsic and adaptive myelination-A sequential mechanism for smart wiring in the brain. Dev Neurobiol 2018;78:68–79
42. Yeung MS, Zdunek S, Bergmann O, et al. Dynamics of oligodendrocyte generation and myelination in the human brain. Cell 2014;159:766–74
43. Dimou L, Simons M. Diversity of oligodendrocytes and their progenitors. Curr Opin Neurobiol 2017;47:73–9
44. Jakel S, Agirre E, Mendanha FA, et al. Altered human oligodendrocyte heterogeneity in multiple sclerosis. Nature 2019;566:543–7
45. Timmler S, Simons M. Grey matter myelination. Glia 2019;67:2063–70
46. Donkels C, Peters M, Farina Nunez MT, et al. Oligodendrocyte lineage and myelination are compromised in the gray matter of focal cortical dysplasia type IIa. Epilepsia 2020;61:171–84
47. Reyes A, Kaestner E, Bahrami N, et al. Cognitive phenotypes in temporal lobe epilepsy are associated with distinct patterns of white matter network abnormalities. Neurology 2019;92:e1957–e68
48. Baumer FM, Peters JM, Clancy S, et al. Corpus callosum white matter diffusivity reflects cumulative neurological comorbidity in tuberous sclerosis complex. Cereb Cortex 2018;28:3665–72
49. Bells S, Lefebvre J, Longoni G, et al. White matter plasticity and maturation in human cognition. Glia 2019;67:2020–37

50. Moavero R, Benvenuto A, Emberti Gialloreti L, et al. Early clinical predictors of autism spectrum disorder in infants with tuberous sclerosis complex: Results from the EPISTOP study. J Clin Med 2019;8.
51. Gould RM, Freund CM, Palmer F, et al. Messenger RNAs located in myelin sheath assembly sites. J Neurochem 2002;75:1834–44
52. Schafer I, Muller C, Luhmann HJ, et al. MOBP levels are regulated by Fyn kinase and affect the morphological differentiation of oligodendrocytes. J Cell Sci 2016;129:930–42
53. Richetto J, Chesters R, Cattaneo A, et al. Genome-wide transcriptional profiling and structural magnetic resonance imaging in the maternal immune activation model of neurodevelopmental disorders. Cereb Cortex 2017;27:3397–413
54. Prohl AK, Scherrer B, Tomas-Fernandez X, et al. Early white matter development is abnormal in tuberous sclerosis complex patients who develop autism spectrum disorder. J Neurodev Disord 2019;11:36.